Experimental Study and Modeling of Surge and Swab Pressures in Horizontal and Inclined Wells

Ruchir Srivastav, Superior Energy Services, University of Oklahoma; Ramadan Ahmed, University of Oklahoma and Arild Saasen, University of Stavanger

Abstract

With increasing eccentricity, surge and swab pressures will be considerably reduced during tripping operations. Therefore, ignoring the pipe eccentricity can result in unnecessarily reduced tripping speed and thus increased operating time. This article presents a new hydraulic model that accounts for eccentricity in surge and swab pressure predictions. Moreover, it presents results of modeling and experimental studies conducted on surge and swab pressures in eccentric annuli with Herschel Buckley fluid. The model assumes close-ended pipe that moves axially at a constant speed. It approximates the flow in eccentric annulus to several hydraulically equivalent concentric annuli sectors with variable annular clearance. To validate the model, experimental investigations were carried out using a 12-ft long vertical annular (1.32" × 2") test section. Pipe trip speed, eccentricity and test fluid formulation were varied during the investigation. Different formulations of polymer based fluids were used in the experiments.

For both concentric and eccentric annuli, the comparison of experimental measurements with model predictions shows good agreement with maximum discrepancy of 14%. Furthermore, parametric study was conducted to examine the effects of well diameter ratio, eccentricity and fluid rheological properties on surge pressure. Substantial decrease in surge pressure (maximum 40% reduction) was observed with increase in eccentricity. The outcomes and findings of this study are useful to perform optimization using the hydraulic models. The optimization is essential in planning of horizontal and extended reach wells in which wellbore pressure management is very critical and no high speed telemetry is used in the well.

1. Introduction

Deep-water drilling has rapidly evolved in the recent past. Current progressions in technology have ensued in more complex drilling operations (highly deviated, extended reach and horizontal wells), and results in more difficult bottomhole pressure management. Moreover, with enhanced use of technologies like slim-hole and casing while drilling and casing running operations results is excessive surge pressure conditions. Failing to identify these down-hole pressure fluctuations, it can result in drilling problems including fracturing of formation, lost circulation, kicks and blowouts. Mitigation of the problems directly results in increased budgets due to non-productive times, damages to equipment and expensive corrective actions. Hence, an accurate surge pressure model is required to effectively predict tripping and casing running speed limits.

Several studies have been conducted to accurately determine surge and swab pressures to optimize tripping operations. However, most of the studies have been conducted for a concentric annulus.

Eccentricity is an essential element when accounting for pressure surge in inclined wells. Few studies (Hussain and Sharif 1997) have been conducted that investigate the effects of eccentricity on pressure surge. Numerical results showed considerable (as high as 35%) reduction in surge pressure due to eccentricity. In addition, the studies were conducted considering commonly used rheology models such as: Newtonian, Bingham plastic and power law models. However, recent studies show that the yield power law (Herschel Buckley) model best describe the fluid flow characteristics of most of fluids used in drilling and completion operations. Therefore, studying flow behavior of yield power law (YPL) fluids in eccentric annulus during tripping operation is very important.

This study discusses a novel steady-state model to calculate surge and swab pressures in eccentric annuli. The model uses an approximation technique that discretizes eccentric annulus into several concentric annuli sectors with varying annular clearance. Each discretized annulus is solved utilizing a set of non-linear equations. A program (Visual Basic code) was developed to solve for the non-linear equations and predict the surge pressure in eccentric annulus.

In this study, experiments were performed to investigate the effects of fluid theology and eccentricity on surge

pressure. Tests were conducted using a setup that has casing as a 2-inch polycarbonate tube and the inner drillstring was a 1.32-inch steel pipe, having a stroke length of 67 inches. The pipe trip speed was varied to measure surge pressure in both concentric and eccentric annuli. Two polymers (Polyanionic Cellulose and Xanthan gum) were used to prepare test fluids. For both concentric and eccentric annuli, the comparison of experimental measurements with model predictions shows good agreement (maximum discrepancy of 14 %). The effects of tripping speeds, diameter ratios, fluid viscosity and eccentricity on surge pressure were measured as a parametric study and concluded that these variables significantly affect the downhole pressure variations. Experimental results showed substantial decrease in surge pressure (maximum 40% reduction) with increase in eccentricity.

2. Literature Review
Early laboratory and field studies related with surge and swab pressures have been as early as the 1930's, associated with wellbore problems (Cannon 1934; Horn 1950; Goins et al. 1951) like formation fracture, kick, lost circulation due to pressure variations during tripping operations. In early second half of the 20th century few studies attempted to explain the causes of surge and swab pressures. Some studies utilized quantitative techniques to predict pressure variations downhole accounting for only the viscous drag and stationary pipe wall (Cardwell 1953; Ormsby 1954) for Newtonian fluids in both laminar and turbulent flow regimes. Field or recorded pressure is often unavailable; however, few analysis have gathered relevant (**Fig. 1**) data (Burkhardt 1961; Ramsey et al. 1983; Wagner et al. 1993; White et al. 1997) to confirm downhole pressure variations.
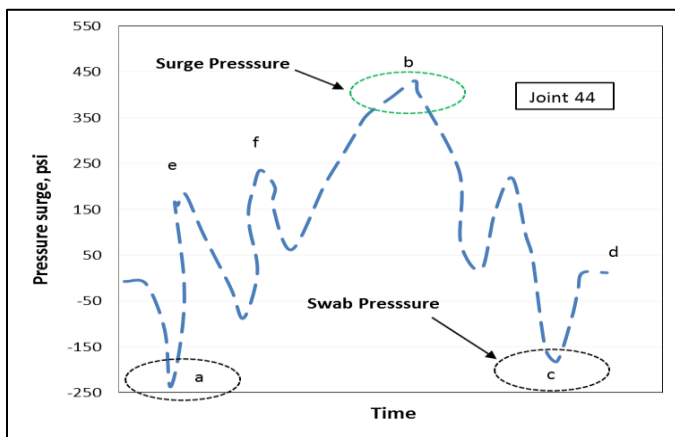

Figure 1: Surge and swab pressures while lowering a casing joint (re-drawn from Burkhardt 1961)

3. Existing Models
Numerous models with continuous advancements to account for all possible consequences that add to pressure variations downhole have been made, to predict these deviations as accurately as possible. Early models were steady state and were only valid for pressure losses in a static pipe due to

viscous forces. Models for Bingham Plastic (Clark 1955; Burkhardt 1961; Clark and Fontenot 1974) and Power law fluids (Schuh 1964) were also developed and accounted for pipe movements. These models were developed considering concentric annular geometry and a close ended drillstring. The developed models were enhanced and implemented into computer programs (Clark and Fontenot 1974).

More recent models accounted for the hydraulic aspect of annular flow with axial inner pipe movement (Chukwu and Blick 1989; Haige and Xishneg 1996; Filip and David 2003). With limitations, many analytical solutions (Malik and Shenoy 1991) and numerical procedures (Lin and Hsu 1980) have also been presented and require further study.

Wellbore geometry and fluid rheology are major factors contributing to pressure variations during tripping operations. Utilizing different diameter ratios (d_p/d_h) as a function of dimensionless flowrate ($\bar{Q}$) (**Fig. 2**) and dimensionless pressure gradient (P) (Chukwu and Blick 1989) for Power Law fluids. Few other limited application models (Malik and Shenoy 1991; Haige and Xisheng 1996) have also been developed for surge pressures.
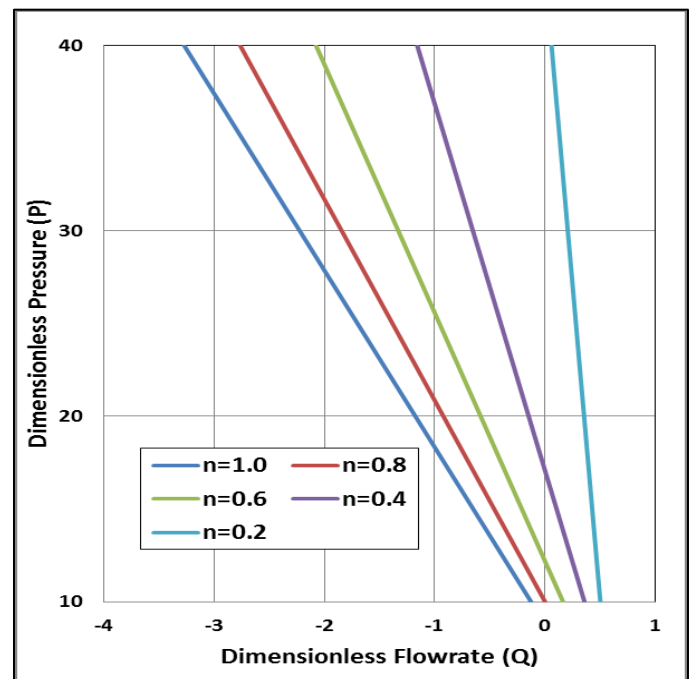

Figure 2: Pressure surge determination for a diameter ratio of 0.2 utilizing a dimensionless pressure gradient plot (data from chukwu and blick 1989)

Limited work has been done to study and investigate the annular velocity profiles in eccentric annulus. Vaughn (1965) presented a study for power law fluids in narrow eccentric annulus. Later, an empirical laminar flow model for Bingham plastic fluid was developed (Walton and Bittleston 1991). Hydraulic models utilizing the concept of equivalent slot have been discussed later and were in good agreement with available data. Haciislamoglu and Langlinais (1991)

developed an exact numerical model to determine the pressure loss reduction due to eccentricity (reduction factor). The reduction factor (R) depends on diameter ratio (K) and fluid behavior index (n). They also examined the effects of axial pipe and yield stress. The study showed that the trip speed has little effect on pressure loss for fluids with yield stress. For stationary inner pipe, the pressure loss in eccentric annulus is computed for the pressure loss of a concentric annulus using the reduction factor as:

$$\left(\frac{dp}{dl}\right)_e = R \times \left(\frac{dp}{dl}\right)_c \qquad (1)$$

$$R = 1 - 0.72\frac{e}{n}\left[\frac{d_p}{d_h}\right]^{0.8454} - 1.5e^2\sqrt{n}\left[\frac{d_p}{d_h}\right]^{0.1852} +$$

$$0.96e^3\sqrt{n}\left[\frac{d_p}{d_h}\right]^{0.2527} \quad\dots\dots\dots\dots\dots\dots\dots\dots\dots\dots (1)$$

Figure 3 shows velocity profiles of Bingham plastic fluid in concentric and eccentric annuli (Haciislamoglu and Langlinais, 1990). Majority of eccentric annulus studies are based on experimentally measured annular pressure obtained by varying hole geometry and fluid type. A number of studies (Singh and Samuel 1999; Saluja 2003; Ogugbue and Shah 2011) used CFD simulations to predict pressure losses in annular sections.

Few studies (Bing et al. 1995; Yang & Chukwu 1995a; 1995b Hussian and Sharif, 1997) adopted couette flow (laminar flow between stationary and moving plates) models to forecast pressure variations. Yang and Chukwu (1995a) presented their results in dimensionless form.
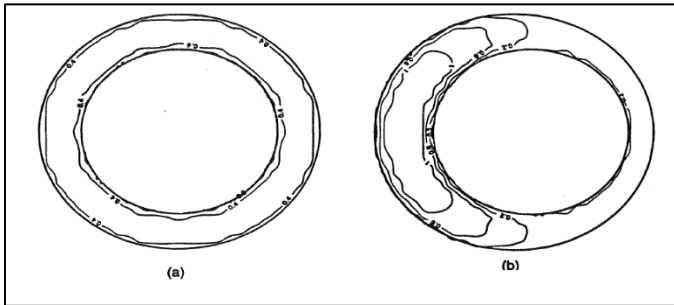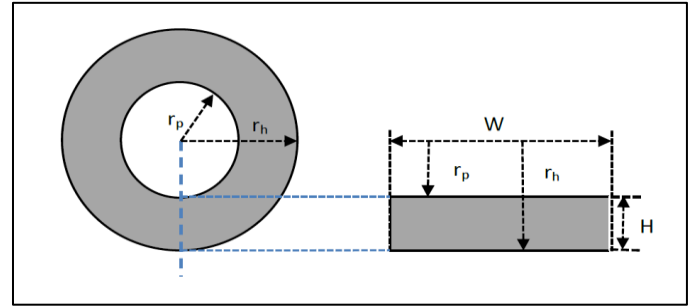

Figure 3: Concentric and Eccentric annulus – Velocity Profile Distribution (Haciislamoglu and Langlinais, 1990)

More recently, unsteady state surge pressure models (Lal 1983; Bing et. al 1995) that account for acceleration have been developed Other studies (Lubinski et al. 1977; Lal 1983; Mitchell 1988) considered fluid inertia, fluid and wellbore compressibility, and pipe elasticity. In general, steady state models under-predict surge and swab pressures as they neglect transient effects. Crespo et al. (2012) developed improved steady state model, which accounts for fluid and wellbore compressibility, and pipe elasticity.

The preliminary experimental results of Srivastav et al. (2012) show the effect of eccentricity on surge and swab pressures. Recently, a number of modeling studies (Tang et al. 2016a; 2016b; He et al. 2016) have been conducted to predict surge pressure in eccentric and partially locked annuli.

3.1 Concept of Narrow-Slot Model
To simplify the mathematical analysis of annular flow, a number of approximate models have been developed considering different fluid rheology models such as Newtonian, Bingham Plastic, power law and yield power law (Guillot and Dennis 1988; Chukwu and Blick 1989; Guillot 1990; Bourgoyne et al. 1986; Crespo et al. 2010; Crespo 2011). One of the models commonly used in the industry is the narrow-slot model, which approximates a concentric annulus by an equivalent slot (**Fig. 4**).
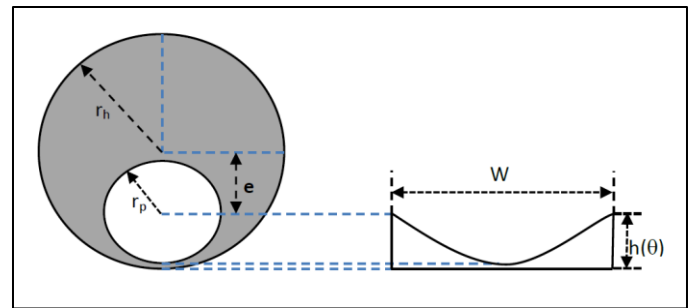

Figure 4: Equivalent slot representation of concenteric annulus (Srivastav 2013)

Eccentricity is an important factor for the determination of pressure variations due to tripping operations. In horizontal or inclined conditions, the pipe may lay on the low side of the wellbore. Models developed concentric annuli over-predict surge pressure in horizontal and inclined wells.

4. Model Formulation
In this study, the narrow-slot modeling technique developed by Iyoho and Azhar (1981) has been adopted to predict surge and swab pressures. The eccentric annulus is divided into numerous concentric annuli with a variable annular clearance. Each concentric annulus is treated separately and represented by its annular clearance, which is a function of pipe eccentricity and angular position (**Fig. 5**).

Figure 5: Equivalent slot representation of eccentric annulus (Srivastav 2013)

The annular flow is as a result of mud displacement induced by the inner pipe movement. The surge flow in concentric annuli is modeled as a narrow slot, which is represented by a movement plate (drillpipe) that travels at a

constant velocity V_p and stationary plate (hole or casing). The following assumptions were presumed during the model formulation:

- The fluid is incompressible (constant density);
- Steady state and isothermal Couette flow conditions;
- Laminar flow;
- Drillpipe moving at a constant speed, V_p;
- Negligible wall slippage effects.

Figure 6 illustrates the representation of an eccentric annulus by variable slot geometry. Flow in each discretized section is solved as a narrow slot with a constant slot height of h, which is a function of angular position (θ) and eccentricity. The expression for the slot height (Iyoho and Azar 1981) is given as:

$$h(\theta) = (r_o^2 - \varepsilon^2 c^2 sin^2\theta)^{0.5} - r_i + \varepsilon c cos\theta \quad \text{.......} \quad (2)$$

where, ε is fractional eccentricity, which is calculated as: $\varepsilon = e/c$, where c is the radial difference and e is offset distance between pipe and borehole centers.
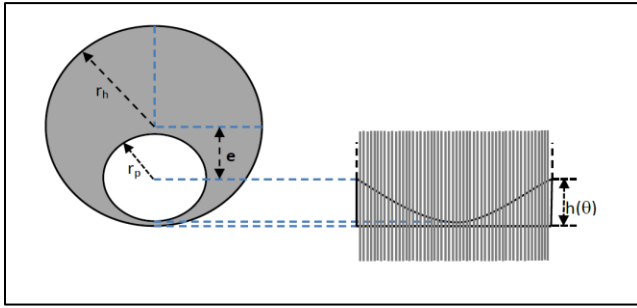
Figure 6: Discretized variable narrow slot into approximated concentric annuli (Srivastav 2013)

Crespo (2011) developed model flow equations to represent velocity profiles for (**Fig. 7**) YPL fluid in concentric annulus with inner pipe axial motion. The velocity distribution has three distinct flow regions:

- Region I, the outer sheared region (0 ≤ y ≤ y1);
- Region II, the plug zone region (y1 ≤ y ≤ y2);
- Region III, the inner sheared region (y2 ≤ y ≤ h)
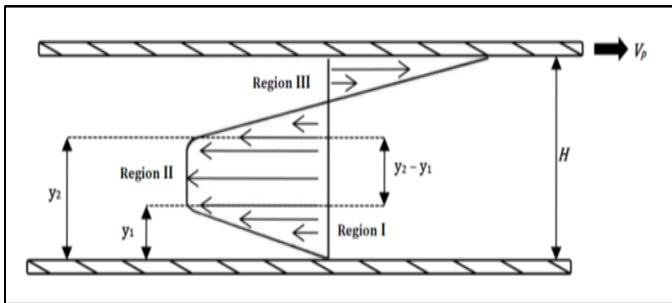
Figure 7: Yield power law velocity profile distribution through a narrow slot (Crespo 2011)

Dimensionless surge pressure (π_1) and dimensionless exponent (b) used in model development are expressed as:

$$\pi_1 = \left(\frac{n}{n+1}\right)\left(\frac{h}{V_p}\right)\left(\frac{\Delta P}{\Delta L}\frac{h}{k}\right)^{\frac{1}{n}} \quad \text{............…..........} \quad (3)$$

$$b = \frac{n+1}{n} \quad \text{...} \quad (4)$$

The dimensionless plug thickness (π_2) is determined from the dimensionless plug-boundary limits ($\bar{y}_1$ and $\bar{y}_2$) as:

$$\pi_2 = \bar{y}_2 - \bar{y}_1 \quad \text{..............…....................} \quad (5)$$

The dimensionless plug-boundary limits are obtained from plug-boundary limits as:

$$\bar{y}_1 = \frac{y_1}{h} \quad and \quad \bar{y}_2 = \frac{y_2}{h} \quad \text{..................................} \quad (6)$$

Applying momentum balance (Crespo 2011), and relationship can be established between dimensionless plug thickness and surge pressure gradient as:

$$\pi_2 = \frac{2\tau_o/h}{\Delta P/\Delta L} \quad \text{......................................} \quad (7)$$

From Fig. 7, if the velocity gradient in Region I is negative, then it will be positive in Region III. The velocity at $\bar{y}_1$ and $\bar{y}_2$ must be equal, as the velocity in the plugged zone is uniform; therefore, $\bar{V}_1$ and $\bar{V}_2$ must be same at these localized points. Thus:

$$(1 - \bar{y}_1 - \pi_2)^b - (\bar{y}_1)^b - \frac{1}{\pi_1} = 0 \quad \text{...............} \quad (8)$$

4.1 Flowrate Analysis

The total dimensionless flow rate is the sum of individual flow rates for each region. Therefore:

$$\bar{q}_t = \int_0^1 (\bar{V}_1 d\bar{y} + \bar{V}_2 d\bar{y} + \bar{V}_3 d\bar{y}) \, dx \quad \text{...................} \quad (9)$$

where, $\bar{q}_t$ is dimensionless total flow rate and is expressed as

$$\bar{q}_t = \frac{-q}{WHV_p} \quad \text{...} \quad (10)$$

Inserting the values of dimensionless velocities into Eq. (9) and integrating, the following dimensionless expression can be established for computing flow rate (Crespo 2011):

$$\bar{q}_t = -\pi_1 \left[\left(\frac{b}{b+1}\right)\bar{y}_1^{\,b+1}\right] - [\pi_1(1 - \bar{y}_1 - \pi_2)^b - 1][1 - \bar{y}_1 - \pi_2] + \pi_1 \left(\frac{1}{b+1}\right)(1 - \bar{y}_1 - \pi_2)^{b+1} - \pi_1 (\bar{y}_1)^b \pi_2 \quad \text{.....................................} \quad (11)$$

For a close-ended pipe, the annular flow rate is amount of fluid being displaced during tripping operations. Neglecting

circulation loss and ballooning effects, the displacement flow rate can be expressed as:

$$q = \frac{\pi}{4} d_p^2 V_p \quad \text{...} \quad (12)$$

To represent the wellbore geometry, annular clearance h(θ) and average slot width (W) are defined as:

$$h = \frac{(d_h - d_p)}{2} \quad \text{...} \quad (13)$$

$$W = \frac{\pi}{2}\left(d_p + d_h\right) \quad \text{...................................} \quad (14)$$

Therefore, Eqn. (10) can be combined with Eqns. (12), (13) and (14) to yield the following model equation.

$$\bar{q}_t = \frac{-1}{\left(\frac{d_h}{d_p}\right)^2 - 1} \quad \text{...............................} \quad (15)$$

Hence, Eqn. (11) can be re-written as:

$$\frac{-1}{\left(\frac{d_h}{d_p}\right)^2 - 1} = -\pi_1\left[\left(\frac{b}{b+1}\right)\bar{y}_1^{b+1}\right] - [\pi_1(1 - \bar{y}_1 - \pi_2)^b -$$

$$1][1 - \bar{y}_1 - \pi_2] + \pi_1\left(\frac{1}{b+1}\right)(1 - \bar{y}_1 - \pi_2)^{b+1} -$$

$$\pi_1\,(\bar{y}_1)^b \pi_2 \quad \text{...} \quad (16)$$

4.2 Modeling Flow in Eccentric Annulus
From previous discussions, eccentric annulus is represented by several narrow slots with variable clearance (h). The annulus is divided into 360 segments of 1° each with clearance calculated (Eqn. 2) at the mid-point of each segment. Utilizing the calculated height (h), the outer diameter is calculated by rearranging Eqn. (13) and dimensionless flowrate is calculated as defined by Eqn. (11). Due to symmetry, the calculation was performed for half of the annulus. The modified equations are summarized below for individual segment calculations. After the slot height calculation, an iterative technique is utilized for a given pressure gradient, which is systematically varied until all model equations are satisfied. A computer program has been developed to solve the problem numerically.

$$d_h(\theta) = 2h(\theta) + d_p \quad \text{.............................} \quad (17)$$

$$\pi_1(\theta) = \left(\frac{n}{n+1}\right)\left(\frac{h(\theta)}{V_p}\right)\left(\frac{\Delta P}{\Delta L}\frac{h(\theta)}{k}\right)^{\frac{1}{n}} \quad \text{...............} \quad (18)$$

$$\pi_2(\theta) = \frac{2\tau_o / h(\theta)}{\Delta P / \Delta L} \quad \text{.............................} \quad (19)$$

$$\bar{q}_t(\theta) = -\pi_{1\,(\theta)}\left[\left(\frac{b}{b+1}\right)\bar{y}_1^{b+1}\right] - [\pi_1(\theta)(1 - \bar{y}_1 -$$

$$\pi_2(\theta))^b - 1][1 - \bar{y}_1 - \pi_2(\theta)] + \pi_1(\theta)\left(\frac{1}{b+1}\right)(1 - \bar{y}_1 -$$

$$\pi_2(\theta))^{b+1} - \pi_1(\theta)\,(\bar{y}_1)^b \pi_2(\theta) \quad \text{.......................} \quad (20)$$

Hence, the following expression provides the total annular flowrate in dimensionless form as:

$$\bar{q}_{total} = 2 \times \sum_{1}^{\theta=180} \bar{q}_t\,(\theta) \quad \text{.......................} \quad (21)$$

Limiting Values of $\bar{y}_1, \bar{y}_2$ and π_2
As shown in Fig. 7, the maximum possible value for y_2 is H, which becomes 1 in dimensionless form. During model development, it has been identified that, at higher eccentricity values, inaccuracy in $\bar{y}_2$ becomes substantial. Hence, a check has been included and the maximum value of $\bar{y}_2$ is maintained at 1. Similarly, the minimum value of $\bar{y}_1$ is set to 0. Therefore, using Eqn. (16):

$$\pi_{2,max} = \bar{y}_{2,max} - \bar{y}_{1,min} \quad \text{.......................} \quad (22)$$

With the above expression, it is evident that the maximum possible value of $\pi_{2,max}$ is 1. This can be explained as a large percentage of the fluid flows as a plug in the annulus. This occurs when eccentricity is high.

Circumferential Wall Shear Stress Variation
Eccentric annulus has been modeled (Luo and Peden 1990) as a number of concentric annuli with variable outer radius. This approach only considers radial variations in shear stress. Hence, with increasing eccentricity, the circumferential shear stress variation in each sector becomes significant. For purely axial annular flow of power law fluid, comparison of model predictions with exact numerical solutions showed a maximum deviation of 30% (Ahmed and Miska 2009) as model tends to under-predict the pressure loss. In the limiting case of the concentric annulus, the model shows good agreement with analytical and numerical results. Ahmed and Miska (2009) accounted for the circumferential shear stress variations by developing a correction factor as shown in Eqn. (23).

$$\left(\frac{dp}{dl}\right)_{corrected} = \frac{1}{K^{0.27\varepsilon}}\left(\frac{dp}{dl}\right)_{model} \quad \text{...............} \quad (23)$$

where K and ε are the diameter ratio and fractional eccentricity, respectively, where $K = d_p/d_h$. The maximum discrepancy in pressure loss prediction reduces to 8% (Ahmed and Miska 2009) with incorporation of the correction factor. A numerical procedure used to calculate the surge pressure is presented elsewhere (Srivastav 2013).

Model Predictions
The model developed in this study is utilized to generate results for different fluids. These included two fluids used in the experimental study and few hypothetical fluids. In the experimental study, the diameter ratio was 0.66 whereas for hypothetical cases, diameter ratio of 0.73 is used. The tripping speed is varied between 0.1 to 3 ft/s for the hypothetical cases. **Table 1** shows the rheological parameters of the fluids used in the analysis. The flow curves for the experimental fluids are presented in the experimental study part.

Table 1: Rheology fluids considered in the analysis

Fluid Type	Test Fluid	τ_o (lb$_f$/100ft^2)	k (lb$_f$.s^n/100ft^2)	n
Newtonian	F1	0.00	0.8	1.00
Bingham Plastic	F2	6.64	0.8	1.00
Power Law	F3	0.00	0.8	0.50
Power Law	1% PAC	0.00	2.77	0.63
Yield Power Law	F4	6.64	0.8	0.50
Yield Power Law	1% Xanthan Gum	20.90	6.41	0.33

Figures 8-13 show model predictions for fluids presented in Table 1. For Newtonian fluid, expected surge pressure trend with trip speed is observed (Fig. 8). This is consistent with flow in circular pipes, in which the pressure loss is a linear function of mean velocity under laminar flow condition. Results of Bingham plastic fluid (Fig. 9) also demonstrate the expected straight line trend with positive intercept indicating yielding behavior of the fluid. Thus, before the fluid begins to flow, the surge pressure gradient needs to overcome the yield stress (τ_o) value which is represented by the intercept.

Figures 10 and **11** present surge pressure predictions for Power law fluids (F3 and 1% PAC –Polyanionic Cellulose). The fluid flow characteristics are defined by fluid consistency index (k) and fluid behavior index (n). The surge pressure curves are strongly affected by fluid parameter, n, which determines non-linearity of the curves. Due to their shear thinning behavior, surge pressure is not very sensitive to the change in trip speed as it is observed with Newtonian fluid. From the figures, it is also evident that with increasing eccentricity surge pressure decreases considerably. Both fluid parameters (k and n) contribute to downhole pressure variations. The diameter ratio (K) is another factor that influences surge pressure and will be discussed later.
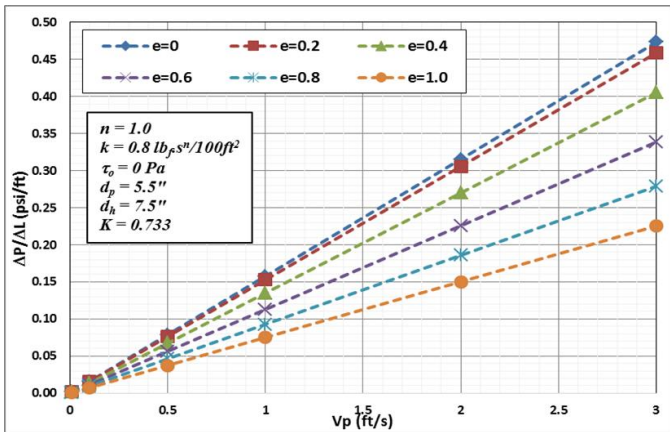
Figure 8: Fluid F1 model predictions
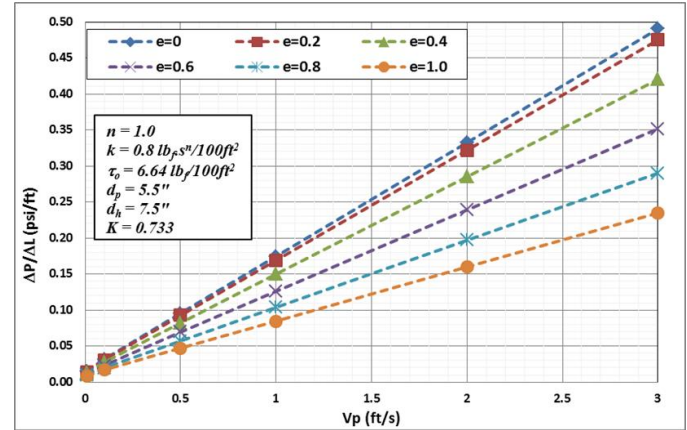
Figure 9: Fluid F2 model predictions
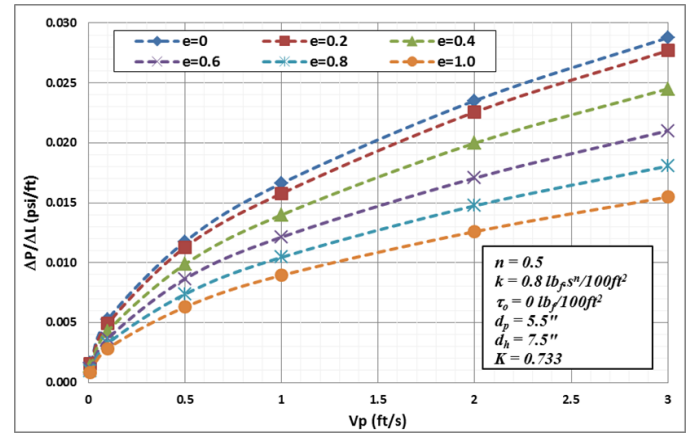
Figure 10: Fluid F3 model predictions
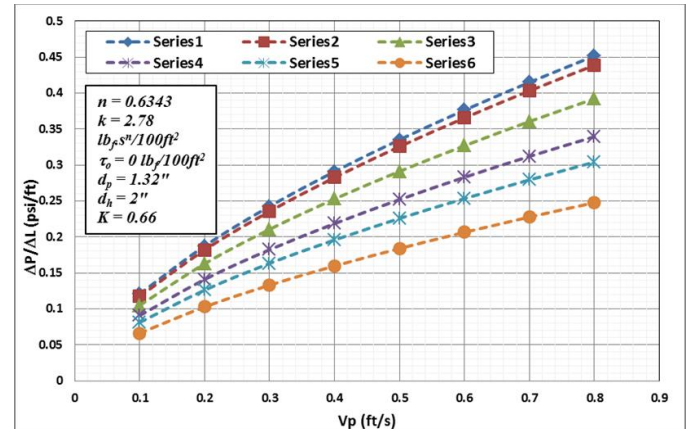
Figure 11: Fluid 1% PAC model predictions

Like Bingham plastic fluids, Yield power law fluids (F4 and 1% Xanthan gum) need minimum pressure gradient to overcome the yield stress and initiate the flow (**Figs. 12** and **13**). At higher pipe velocities, the effect of trip speed diminishes due to significant shear thinning. Surge pressure depicted reducing trend with increasing eccentricity. As shown in Fig. 12, to generate the same level of surge pressure the trip speed has to be tripled in 60% eccentric annulus.
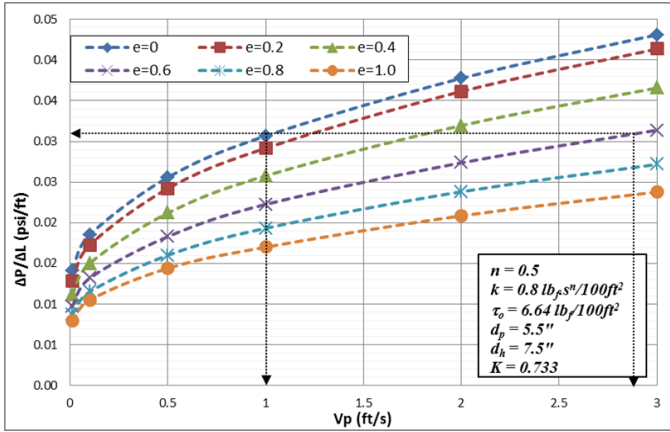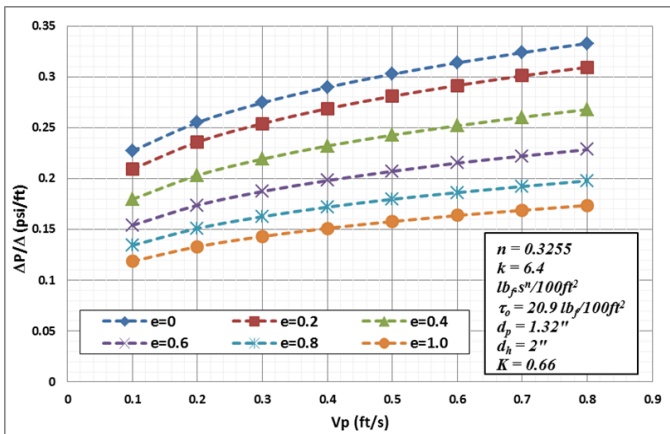
Figure 12: Fluid F4 model predictions

Figure 13: Fluid 1% Xanthan Gum model predictions

5. Experimental Study

The main objective of this study is to examine the effects of different drilling parameters such as trip speed, fluid rheology and eccentricity on surge and swab pressures.

5.1 Experimental Setup

The existing small-scale setup (Crespo 2011) has been improved to satisfy experimental requirements. The tests were performed at ambient conditions in a vertical annulus with proper control of inner pipe axial speed and eccentricity. The setup (**Fig. 14**) has the capability to accurately control trip speed and record measurements. A detailed schematic of the set-up is presented in **Fig. 15**. The set-up includes the following components:

- A 2-inch polycarbonate tube (Casing);
- 1.32-inch inner steel pipe (L = 90 inches);
- Hoisting system: a gearmotor with pulley and cable system to raise and lower the inner pipe at a controlled speed;
- Differential pressure sensor;
- Data acquisition and control system (personal computer and data collection card); and
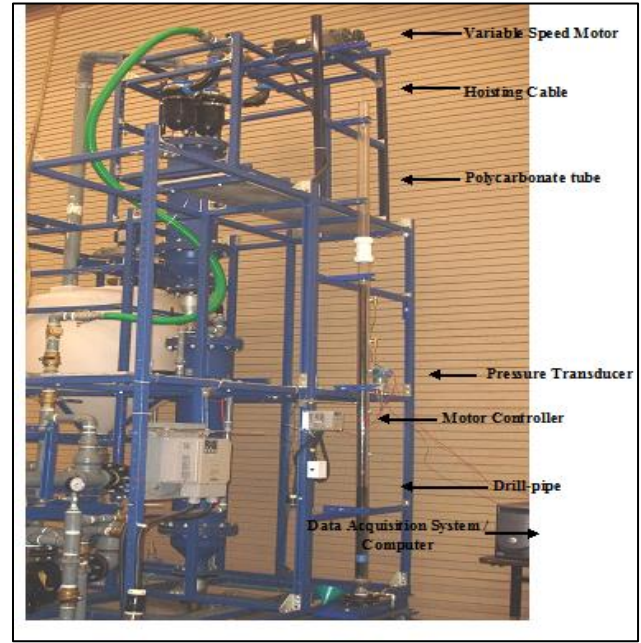- Fluid preparation mixing and collection tanks.

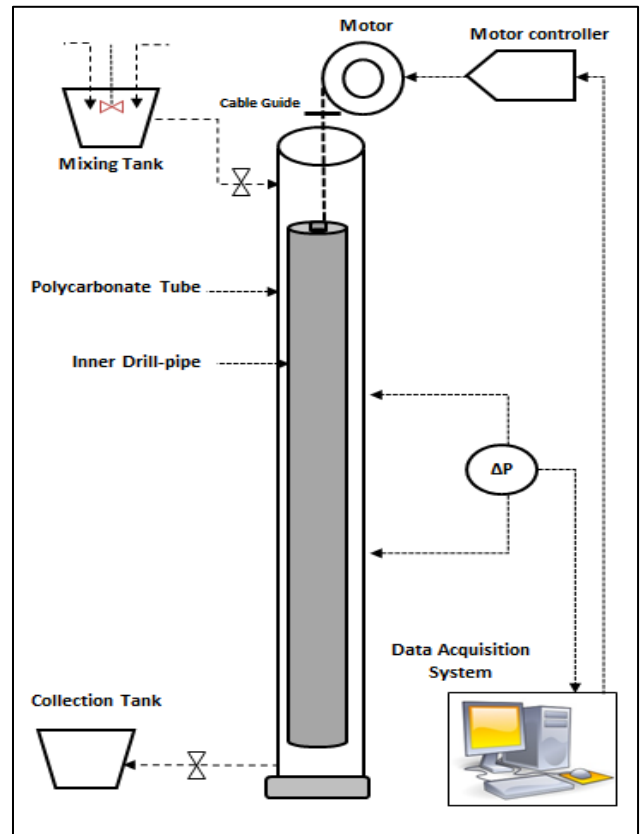**Figure 14: Experimental setup (Srivastav 2013)**

Figure 15: Schematic of experimental setup (Srivastav 2013)

A 148-inch long polycarbonate tube is used as the casing/borehole and attached to the supporting structural frame as show in Fig. 14. The bottom of the tube has a drain valve. The tube is supported by a blind flange at the bottom.

The inner pipe eccentricity was maintained using three screws (**Fig. 16a**), which are placed at the bottom of the inner pipe maintaining 120° apart. The screws were tested for smooth tripping operation. During the experiment, the pipe eccentricity was maintained at about 90% to have a small clearance between the screws that maintain the pipe eccentricity and the casing wall. The clearance reduced the friction and maintained smooth pipe movement during the test.
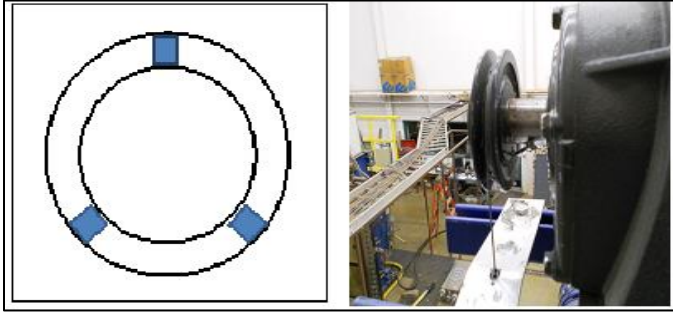

Figure 16:(a) Screws used to maintain eccentricity; (b) Variable speed motor with pulley and cable system (Srivastav 2013)

The hoisting system comprised of a variable speed motor (Fig. 16b) to lift the inner pipe at the desired speed. The maximum trip speed was 1 ft/s with speed controlling accuracy of ±0.01 ft/s. However, the maximum speed limit of the experiments were slightly lower (0.8 ft/s) than 1 ft/s because higher speed require longer stroke length to establish a steady state flow condition. The setup has an effective stroke length of 67 inches and pipe movement is achieved with winding and unwinding of the wire on the pulley as the motor rotated in clockwise and anticlockwise directions.

A differential pressure sensor was connected to the test section to measure surge pressure. It was tested and calibrated prior to performing the experiments. The pressure port tapping distance was 1 ft and the pressure measuring span was 0.0-1.0 psi with an accuracy of ±0.005 psi.

The desired polymeric fluids were prepared in an 8-gallon mixing tank using a variable speed Stirrer (Silverson L4RT). The stirrer was capable of both varying the speed as well as vertical movement that provided more efficient means for mixing and preparing the test fluids. Once the fluids were prepared, they were transferred to the test annular section and experiments were performed. The test started with the inner pipe at the top to attain a full stroke using a hoisting system. The data acquisition system and the pressure transducer were used to record surge pressure data for different tripping speeds. A detailed test procedure is presented elsewhere (Srivastav 2013).

5.2 Test Materials
Experiments were performed varying concentrations of polymeric fluids (Polyanionic Cellulose and Xanthan Gum suspensions). Flow behavior of Polyanionic Cellulose suspensions (PAC) best fits the power law model whereas that of Xanthan gum suspensions best fits the yield power law

model. The tests were performed in concentric and eccentric annuli. Two rotational viscometers (spring factor of 1 and 1/5 respectively) were used to measure rheology of the fluids. Using the polymers, test fluids with different polymer concentrations were prepared and their rheological properties were measured (**Figs. 17** and **18**). Script A is used to identify fluids utilized in concentric annulus test and Script B used to identify fluids utilized in eccentric annulus test. Rheologies of fluids used in concentric annulus test are similar to the rheologies of fluids used in the eccentric annulus test.
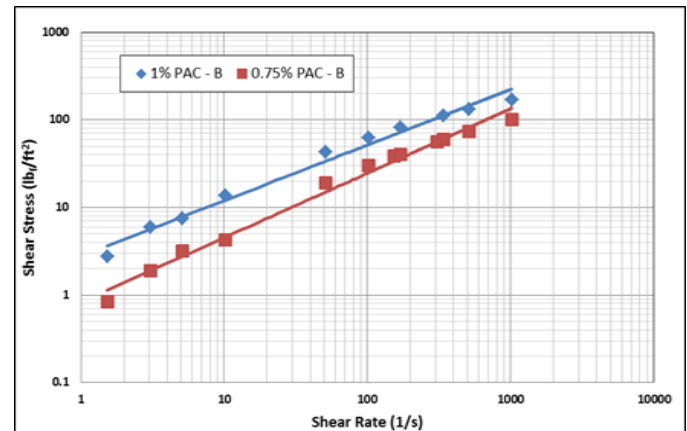

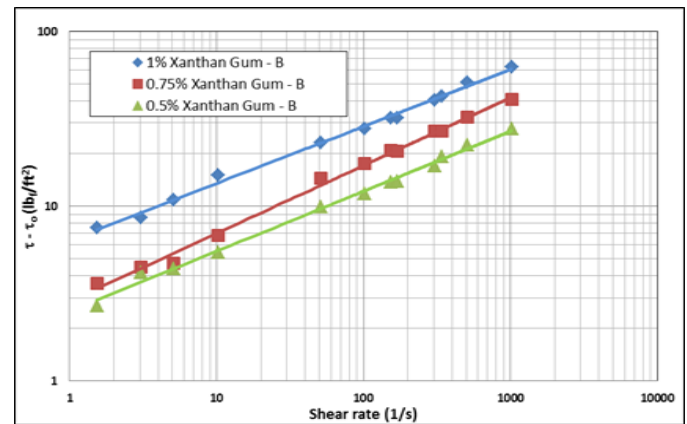**Figure 17: Rheology measurements for PAC based fluids used in eccentric annulus test (Srivastav 2013)**

Figure 18: Rheology measurements for Xanthan gum based fluids used in eccentric annulus test (Srivastav 2013)

5.3 Experimental Results and Model Predictions
For PAC based fluids (power law fluids), model predictions show reasonable agreement with experimental measurements (**Figs. 19** and **20**). The maximum discrepancy between measurements and predictions is 13%, which can be attributed to pipe oscillation at higher tripping speeds and model inaccuracy because of neglecting the circumferential shear stress variations. Although correction factors are introduced in model formulation to account for circumferential shear stress variations, there are still discrepancies due to velocity profile differences. This discrepancy can also be a result of other modeling assumptions.
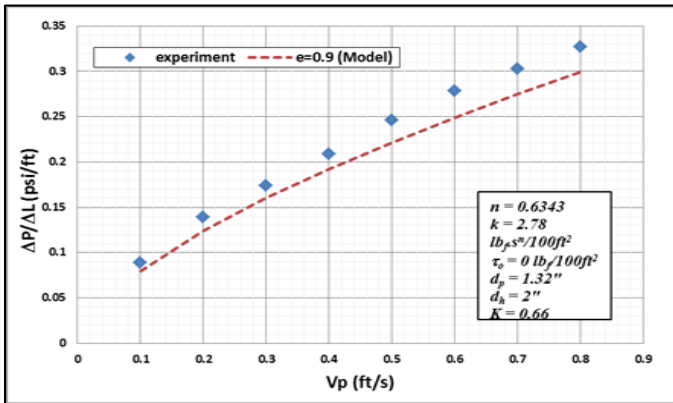
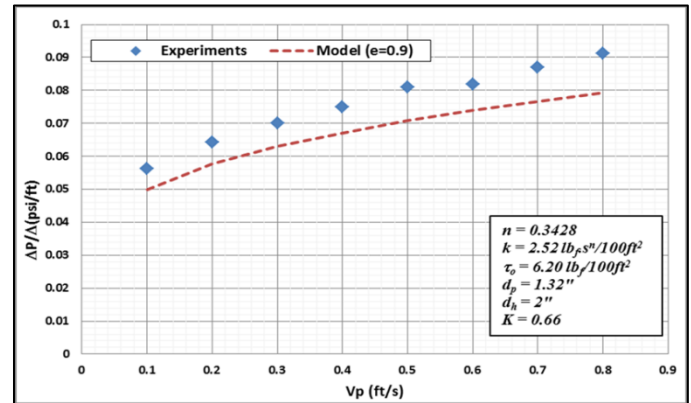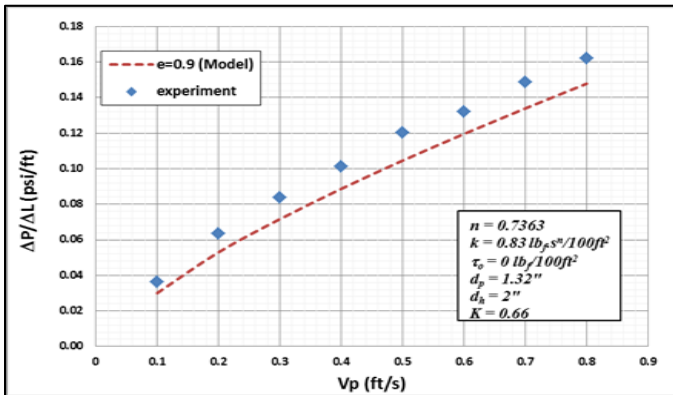**Figure 19: Surge gradient vs. pipe speed for ε = 0.9; PAC 1%**
(Srivastav 2013)

Figure 20: Surge gradient vs. pipe speed for ε = 0.9; PAC 0.5%
(Srivastav 2013)

Figures 21 and **22** compare experimental results with model predictions for Xanthan gum (XG) based fluids, which best fits the YPL rheology model. Model predictions were comparable to experimental results with a maximum discrepancy of 14% at high tripping speeds. The deviation can be attributed to the model weaknesses discussed earlier. It is evident that with decreased viscous propety, there is a gradual reduction in the generated surge pressure.
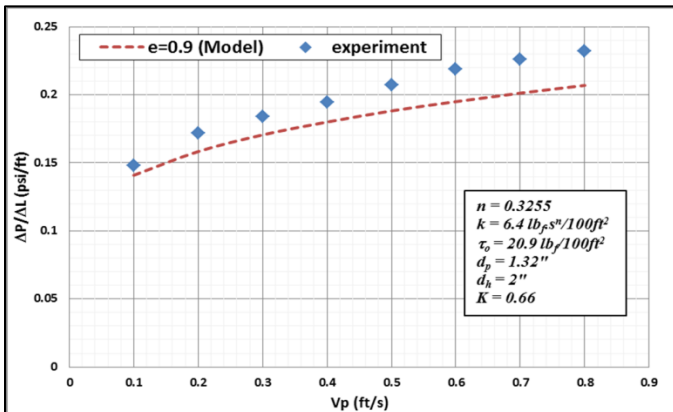

Figure 21: Surge gradient vs. pipe speed; ε = 0.9; XG 1%
(Srivastav 2013)

Figure 22: Surge gradient vs. pipe speed; ε = 0.9; XG 0.5%
(Srivastav 2013)

5.4 Parametric Study

The parametric study is performed between two hypothetical fluids, one being power law fluid while other being yield-power law fluid. The only rheological difference between the two fluids is yield stress of the YPL fluid. The effects of diameter ratios for both concentric and eccentric annulus are studied. The casing diameter is kept constant while the inner pipe diameter is varied. The fluid parameters and diameter ratios used during the study are shown in **Table 2**.

Table 2: Fluid type and diameter ratios used for parametric study

Fluid Type	Test fluid	Hole diameter (inches)	Drill-pipe diameter (inches)	Diameter Ratio	Rheological parameters		
					τ_o (Pa)	n	k (Pa.s^n)
Power Law	F5	7.5	3	0.40	0	0.5	0.524
			4	0.53			
			5	0.67			
			6	0.80			
			6.75	0.90			
Yield Power Law	F6	7.5	3	0.40	3.162	0.5	0.524
			4	0.53			
			5	0.67			
			6	0.80			
			6.75	0.90			

Figures 23-26 shows surge pressure predictions as a function of pipe velocity for both concentric and eccentric annulus. It is evident from the figures that, as the surge pressure increases with diameter ratio due to decreased annular clearance. Moreover, surge pressure occurring in concentric annulus significantly higher than the one occurring in eccentric annulus with similar geometry. It can be inferred from the results that, for low diameter ratios, the major contributing factors affecting the surge pressure are the fluid rheological parameters, trip speed and eccentricity. As seen from Figs. 23 and 24, the YPL fluid tends to generate higher pressure surges when compared to a similar flow of power law fluid.
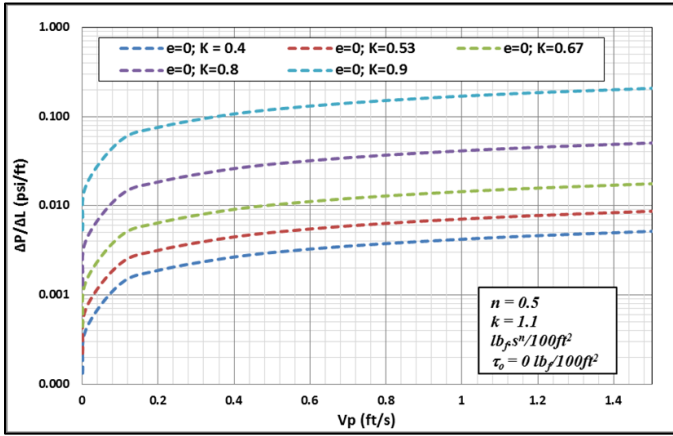
Figure 23: Effect of diameter ratios on surge pressure, Fluid F5 (Srivastav 2013)
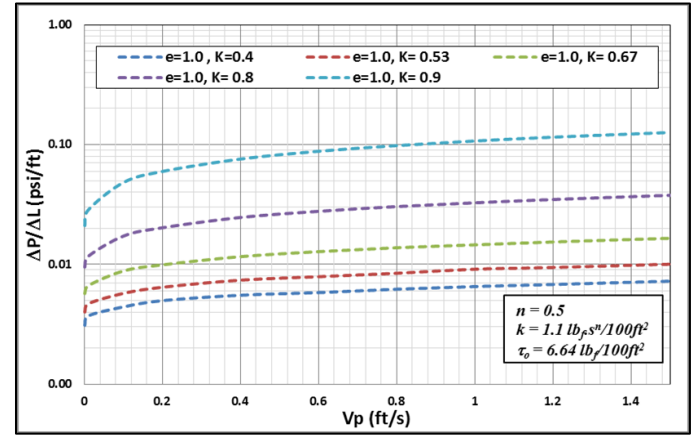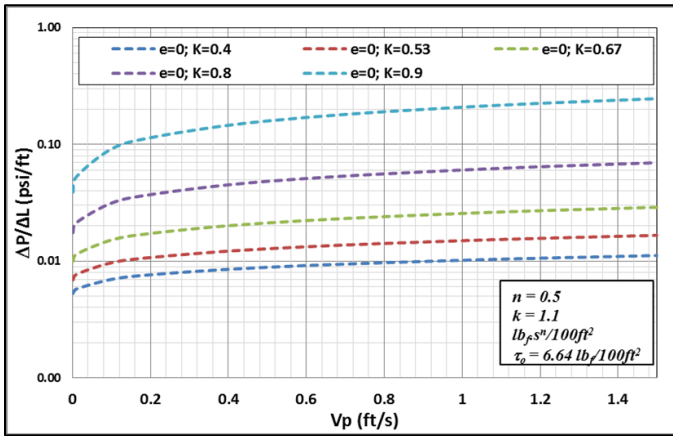

Figure 24: Effect of diameter ratios on surge pressure, Fluid F6 (Srivastav 2013)

Figure 25: Effect of diameter ratios on surge pressure, Fluid F5 (Srivastav 2013)
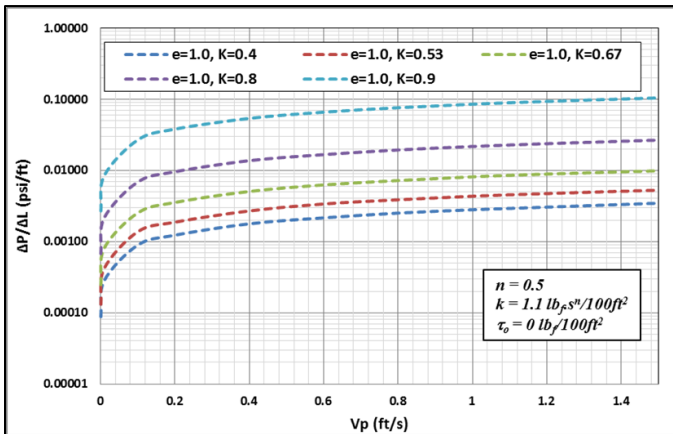

Figure 26: Effect of diameter ratios on surge pressure, Fluid F6 (Srivastav 2013)

5.5 Comparing Concentric and Eccentric Annulus

The experimental measurements and model predictions are presented together to show the reduction in surge pressure due to eccentricity. The maximum surge pressure reduction of 32% (**Fig. 27**) was observed with power law fluid (PAC 0.75%) while reduction of 38% (**Fig. 28**) was occurred with YPL fluid (1% Xanthan gum). The model predictions here provide a useful insight to the effects of eccentricity on surge pressure. The experimental data show smaller reduction in surge pressure than the model predictions. This could be attributed to the pipe lateral movement during the test, which slightly changes the eccentricity of the pipe causing surge pressure reduction in concentric pipe as the pipe tends to move toward the wall and increase in surge pressure as highly eccentric pipe moves toward the center. During the experiment, it was difficult to maintain both fully concentric and fully eccentric pipe configurations. Hence, model predictions for concentric and eccentric annuli can be considered as the limiting boundary for surge pressure of a given fluid and diameter ratio (K), since experimental results were always within the model prediction of concentric and eccentric annulus.
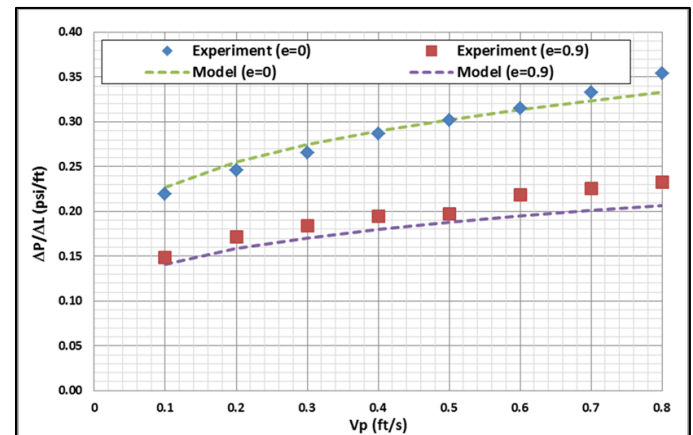

Figure 27: Measured and predicted surge pressures for 1% XG fluid (Srivastav 2013)
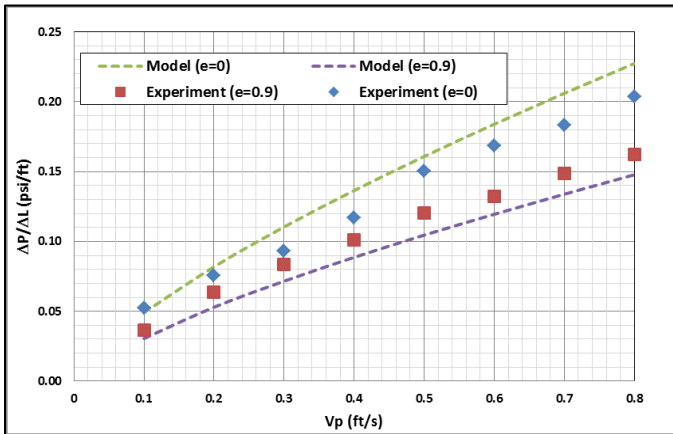
Figure 28: Measured and predicted surge pressures for 0.75% PAC (Srivastav 2013)

Conclusions

The numerical model developed in this study precisely predicts surge and swab pressures simulating downhole pressure fluctuations occurring during tripping in inclined and horizontal wells. The model utilizes the existing variable narrow-slot approximation technique to account for pipe eccentric in surge pressure calculation. Based on the outcomes of this investigation, the following conclusions can be made:

- The present model predicts surge and swab pressures of yield power law fluid in eccentric annulus (i.e. eccentricity ranging from 0 to 90%) with reasonable accuracy (maximum discrepancy of 14%).
- Eccentricity has considerable effects on surge and swab pressures. Both experimental and theoretical results show surge pressure reduction of up to 40% as a result of eccentricity.
- Results show that for highly shear thinning fluids, a small decrease in surge pressure can considerably increase the safe tripping speed limit.
- Surge pressure predictions for concentric and eccentric model can be considered as the boundary limits for the expected surge pressures. In real field condition, due to pipe lateral movement the pipe does not maintain the concentric or fully eccentric geometry throughout, resulting in surge pressure variations between these to limits.
- In general, fluid rheological parameters, tripping speeds and diameter ratios considerably affect the generated pressure surges.

Acknowledgments

Nomenclature

$\bar{q}_t$ = Total dimensionless flow rate
$\bar{q}_t(\theta)$ = Total dimensionless flow rate for the segment
$\bar{P}$ = Surge/Swab pressure
$\bar{q}_{total}$ = Total dimensionless flow rate for all the segments
$\bar{y}_1$ = Dimensionless lower boundary limit of Region II
$\bar{y}_2$ = Dimensionless upper boundary limit of Region II
d_h = Hole/Casing diameter
d_p = Pipe diameter
V_{ms} = Effective mud velocity
V_p = Pipe velocity
V_v = Velocity due to pipe movement
y_1 = Lower limit of Region II
y_2 = Upper limit of Region II
$\bar{K}$ = Clinging Constant
P_s = Surge/Swab pressure
$\bar{Q}$ = Dimensionless flow rate
V_{ae} = Effective annular mud velocity
A_a = Annular area
A_p = Area displaced by drill pipe
b = Constant
c = radial clearance ($r_o - r_i$)
$d_h(\theta)$ = Hole / Casing diameter of the segment for variable slot calculations
e = inner pipe offset from the center
f = friction factor
f_b = Bingham fluid modified friction factor
f_l = laminar flow regime friction factor
f_t = turbulent flow regime friction factor
h = Slot Thickness
$h(\theta)$ = Segment Slot Thickness
k = Consistency Index
L = Length of the wellbore
n = Fluid behavior index
N = Spring factor
q = Actual flow rate
Q_i = drill-pipe flow rate
R = Reduction factor
Re = Reynolds number
r_i = Outer radius of inner pipe
r_o = Inner radius of outer pipe
S = Bingham number / Plasticity
v = Voltage
W = Slot width
K = Diameter ratio (K= d_p/d_h)

Greek Letters

ε = Fractional eccentricity
λ = Conductance number
μ_p = Plastic viscosity
γ_w = Wall shear rate
ρ = Fluid density
π = Pi
π_1 = Dimensionless pressure
$\pi_1(\theta)$ = Dimensionless pressure for the segment

π_2 = Dimensionless plug thickness

$\pi_2(\theta)$ = Dimensionless plug thickness for the segment

ϕ = Correction factor

θ_i = Dial reading

τ = Shear stress

τ_w = Shear stress at the wall

τ_0 = Yield stress

$\frac{dv}{dy}$ = Shear rate

$\frac{dp}{dl}$ = Pressure gradient

ΔL = Slot length/Wellbore depth

ΔP = Pressure drop

Subscripts

h = Hole

p = Pipe

θ = Angle / segment for eccentric annulus discretization

e = eccentric annulus

c = concentric annulus

References

Ahmed, R. and Miska, S. 2009. Advanced Drilling and Well Technology, Chapter 4, Society of Petroleum Engineers, pp217.

Bing, Z., Kaiji, Z. and Qiji, Y. 1995. Equations Help Calculate Surge and Swab Pressures in Inclined Well, Oil & Gas Journal, Vol. 93, pp 74-77, 18 September.

Bourgoyne, A. T. 1986. Applied Drilling Engineering, SPE Textbook Series, Vol. 2, Richardson, Texas, pp. 167-171.

Burkhardt, J. A. 1961. Wellbore Pressure Surges Produced by Pipe Movement, Journal of Petroleum Technology, June, pp 595-605.

Cannon, G. E. 1934. Changes in Hydrostatic Pressure due to Withdrawing Drillpipe from the Hole, API Drilling and Production Practices, pp 42-47.

Cardwell, W. T. 1953. Pressure Changes in Drilling Wells Caused by Pipe Movement, API Drilling and Production Practices, pp 97-112.

Chukwu, G. A. and Blick, E. F. 1989. Couette Flow of Non-Newtonian Power-Law Fluids, Applied Simulation & Modeling, Acta Press, Anaheim, California, 13-15 November.

Clark, E. H. 1956. A Graphic View of Pressure Surges and Lost Circulation, API Drilling & Production Practices, pp 424-438.

Clark, R. K. and Fontenot, J. E. 1974. Field Measurements of the Effects of Drillstring Velocity, Pump Speed and Lost Circulation Material on Downhole Pressures, Paper SPE-4970, presented at the 49th Annual Fall Meeting of the Society of Petroleum Engineers of AIME, Houston, Texas ,6-9 October.

Crespo, F. 2011. Experimental Study and Modeling on Surge and Swab Pressures for Yield-Power-Law drilling fluids, Master's Dissertation Thesis, Mewbourne School of Petroleum & Geological Engineering, University of Oklahoma.

Crespo, F., Ahmed, R. and Saasen, A. 2010. Surge and Swab Pressure Predictions for Yield-Power-Law Drilling Fluids, SPE 138938, SPE Latin American & Caribbean Petroleum Engineering Conference, Lima, Peru, 1-3 December 2010.

Crespo, F., Ahmed, R., Enfis M., Saasen A. and Amani M. 2012. Surge-and-Swab Pressure Predictions for Yield-Power-Law Drilling Fluids, SPE Drilling & Completions, December.

Filip, P. and David, J. 2003. Axial Couette-Poiseuille flow of Power-Law Viscoplastic Fluids in Concentric Annulus, Journal of Petroleum Science and Engineering, Vol. 40, pp. 111 – 119.

Goins, W. C., Weichhert, J. P., Burba, J. L., Dawson, D. D. and

Teplitz, A. J. 1951. Down-the-Hole Pressure Surges and their Effect on Loss of Circulation, API Drilling and Production Practices, pp 125-132.

Guillot, D. 1990. Rheology of Well Cementing Slurries, in E.B. Nelson, Ed., Well Cementing, Schlumberger, Houston, Texas, pp 4:01–37.

Guillot, D. and Dennis, J. D. 1988. Prediction of Laminar and Turbulent Friction Pressures of Cement Slurries in Pipes and Centered Annuli, Paper SPE- 18377, presented at the European Petroleum Conference, London, 18-19 October.

Haciislamoglu, M. and Langlinais, J. 1991. Effect of Pipe Eccentricity on Surge Pressures, Journal of Energy Resources Technology, September, Vol. 113 / 157.

Haige, W. and Xisheng, L. 1996. Study on Surge Pressure for Yield-Pseudoplastic Fluid in a Concentric Annulus, Applied Mathematics and Mechanics, Vol. 17, No. 1, pp 15-23 January.

He, S., Srivastav, R., Tang, M. and Ahmed, R. 2016. A New Simplified Surge and Swab Pressure Model for Yield-Power-Law Drilling Fluids, Journal of Natural Gas Science and Engineering, Volume 28, January 2016, Pages 184–192.

Horn, A. J. 1950. Well Blowouts in California Drilling Operations, Causes and Suggestions for Prevention, API Drilling and Production Practices, pp 112-128.

Hussain, Q. E. and Sharif M. A. R. 2000. Numerical Modeling of Helical Flow of viscoplastic Fluids in eccentric annuli, AIChE Journal, October, Vol. 46, No. 10.

Iyoho A. W. and Azar J. J. 1981. An Accurate Slot-Flow Model for Non-Newtonian Fluid Flow Through Eccentric Annuli, Society of Petroleum Engineers of AIME, October.

Lal, M. 1983. Surge and Swab Modeling for Dynamic Pressures and Safe Trip Velocities, Paper SPE-11412, presented at the IADC/SPE Drilling Conference, New Orleans, Louisiana, 20-23 February.

Lin, S. H. and Hsu, C. C. 1980. Generalized Couette Flow of a Non-Newtonian Fluid in Annuli, Industrial & Chemical Engineering Fundamentals, Vol. 19, No. 4, pp 421-424.

Lubinski, A., Hsu, F. H. and Nolte, K. G. 1977. Transient Pressure Surges Due to Pipe Movement in an Oil Well, Fevue de l'Institut Francais du Petrole, May-June.

Luo, Y. and Peden, J.M. 1990. Flow of Non-Newtonian Fluids through Eccentric annulus, SPE Production Engineering, February.

Malik, R. and Shenoy, U. V. 1991. Generalized Annular Couette Flow of a Power-Law Fluid, Industrial and Engineering Chemical Research, Vol. 30, pp 1950-1954.

Mitchell, R. F. 1988. Dynamic Surge/Swab Pressure Predictions, SPE Drilling Engineering Journal, September, pp 325-333.

Ogugbue, C. C. and Shah, S. N. 2011. Laminar and Turbulent Friction Factors for Annular Flow of Drag-Reducing Polymer Solutions in Coiled-Tubing Operations, SPE Drilling & Completion, December, pp. 506-518

Ormsby, G. S. 1954. Calculation and Control of Mud Pressures in Drilling and Completion Operations, API Drilling and Production Practices, pp 44-55.

Ramsey, M.S., Miller, J.F., Morrison, M.E. and Robinson, L.H. 1983. Bit Hydraulics: Net Pressure Drops Are Lower Than You Think, World Oil, October, pp 65-67.

Saluja, G. 2003. Investigation of CFD Based Simulation for Non-Newtonian Fluid Flow in Concentric and Eccentric Annuli, Master's Dissertation Thesis, Mewbourne School of Petroleum & Geological engineering, University of Oklahoma.

Schuh, F. J. 1964. Computer Makes Surge-Pressure Calculations Useful, Oil & Gas Journal, Vol. 62, No. 31, pp 96-104.

Singh, A. P. and Samuel, R. 2009. Effect of Eccentricity and Rotation on Annular Frictional Pressure Losses with Standoff Devices, SPE-124190, SPE Annual Technical Conference & Exhibition, New Orleans, Louisiana, 4-7 October.

Srivastav, R., Crespo, F., Enfis, M., Ahmed, R., Saasen, A. and Laget, M. 2012. Surge and Swab Pressures in Horizontal and Inclined Wells, SPE-152662, SPE Latin American & Caribbean Petroleum Engineering Conference, Mexico City, Mexico, 16-18 April.

Srivastav, R. 2013. Experimental Study and Modeling on Surge and Swab Pressures in Eccentric Annulus, Master's Dissertation Thesis, Mewbourne School of Petroleum & Geological Engineering, University of Oklahoma.

Tang, M., Ahmed, R. and He, S. 2016a. Simplified Surge Pressure Model for Yield Power Law Fluid in Eccentric Annuli, Journal of Petroleum Science and Engineering, Volume 145, September, 346–356.

Tang, M., Ahmed, R. and He, S. 2016b. Modeling of yield-power-law fluid flow in a partially blocked concentric annulus, Journal of Natural Gas Science and Engineering, Volume 35, Part A, 555–566.

Vaughn, Robert D. 1965, Axial Laminar Flow of Non-Newtonian Fluids in Narrow Eccentric Annuli, SPE 1138, Society of Petroleum Engineers.

Wagner, R. R., Halal, A. S. and Goodman, M. A. 1993. Surge Field Tests Highlight Dynamic Fluid Response, Paper SPE-25771, presented at the IADC/SPE Drilling Conference, Amsterdam (23-25 February).

Walton I.C. and Bittleston S. H. 1991. The axial flow of a Bingham plastic in a narrow eccentric annulus, J. Fluid Mech., Vol 222, pp. 39-60.

White, Z., Zamora, M., and Svodoba, C. 1997. Downhole Measurements of Synthetic-Based Drilling Fluid in an Offshore Well Quantify Dynamic Pressure and Temperature Distributions, SPE Drilling and Completion, pp 149-157 (September).

Yang, L. and Chukwu, G. A. 1995a. Couette Flow of Non-Newtonian Power-Law Fluids in Narrow eccentric Annuli, Ind. Eng. Chem. Res., 34, pp. 936-942.

Yang, L. and Chukwu, G. A. 1995b. A Simplified Couette Flow solution of Non-Newtonian Power-Law Fluids in eccentric annuli, The Canadian Journal of chemical engineering, Volume 73, (April).